Tolerance analysis of surface-to-surface contacts using finite element analysis

Citation for the original published paper (version of record):

Camuz, S., Söderberg, R., Wärmefjord, K. et al (2018). Tolerance analysis of surface-to-surface contacts using finite element analysis. Procedia CIRP, 75: 250-255.
http://dx.doi.org/10.1016/j.procir.2018.04.029

(article starts on next page)

Available online at www.sciencedirect.com

ScienceDirect

Procedia CIRP 75 (2018) 250–255

www.elsevier.com/locate/procedia

15th CIRP Conference on Computer Aided Tolerancing – CIRP CAT 2018

Tolerance Analysis of Surface-to-Surface Contacts Using Finite Element Analysis

Soner Camuz[a], Rikard Söderberg[a], Kristina Wärmefjord[a], Mikael Lundblad[b]

[a]*Dept. Industrial and Materials Science, Chalmers University of Technology, Göteborg, Sweden*
[b]*Metal Cutting Technology, AB Sandvik Coromant, Sandviken, Sweden*

* Soner Camuz Tel.: +46-72-981-99-94.; *E-mail address:* soner@chalmers.se

Abstract

The accuracy of a cutting tool is dependent on the surface-to-surface contact between the tool body and the insert. Depending on the application, the forces generated during a cutting operation will change in both magnitude and direction. This will alter the contact locations between the tool body and carbide insert thus affecting on both tool life and key characteristics such as cutting performance and productivity. In this article, a methodology is presented to analyse contact variation in the interface between the tool body and the carbide insert. Results presented in this paper can be used for tolerance allocation of surface-to-surface contacts.

Peer-review under responsibility of the Scientific Committee of the 15th CIRP Conference on Computer Aided Tolerancing - CIRP CAT 2018.

Keywords: Variation simulation; Machining tool; Tolerances; Contact prediction; Tolerance analysis

1. Introduction

Assembly deviations caused by part variations, fixture variations and external effects such as temperature and mechanical loads are inevitable to avoid and need to be statistically controlled. During the past decades numerous of approaches have been developed in order to handle these type of problems, different approaches for different industries. Within the machining industry research as mainly focused upon fixture design due to the direct response on the produced quality [1]. The most common type of rigid locating method is the $3-2-1$ locating scheme [2] and *N-2-1* for compliant assemblies [3, 4] but it implies that the locators are known and pre-defined. The authors in [5] describe a method using skin-models to address this issue, however, this is purely a rigid assembly variation simulation, which is not applicable for cutting tool assemblies.

Conventional variation simulation of deformable sheet metal assemblies uses Method of Influencing Coefficients (MIC), where a linear relationship between part deviations and the springback deviations is formed [6]. Finite element analysis (FEA) is used on assembly level to calculate springback deviations and extract the stiffness matrix. A novel approach is presented in [7, 8] where a regression model is created for each node of a finite element mesh of an injection moulded plastic part, in order to see the effects of process input parameters, such as mould temperature and cooling time. In [9] a tolerance optimization routine is presented that uses finite element analysis and neural networks to optimize a set of tolerances for a mechanical motor assembly, with respect to manufacturing cost, quality loss and deformation due to inertia effect.

For metal cutting, the locating scheme is given by the contacts between the tool body and insert and the position of the contact points are not always fully constrained. This means that a change of cutting direction or surface topology can affect the contacts between the two bodies. During a cutting operation, depending on the cutting process, the cutting force will change both in magnitude and direction. This will alter the cutting point which will resolve in movements in the carbide insert, thus altering the location and contacts in between the tool body and insert, see Fig. 1a. This can lead to a change in the rake angle, see Fig. 1b, which in a metal removal process can have a dramatical effect on tool life and productivity.

For parting operations there are high demands on the robustness and performance of parting tools due to the fact that during a cut there will be material on both sides of the tool, meaning that chip clearing is crucial. Failure in chip clearing will lead to poor surface qualities and chip jamming that will break the tool. As the tool reaches the center of the work piece the axial forces will drastically increase due to the tangential force going towards zero and the tool is pushing instead of cutting. In [10] the author calculates the cutting forces using finite elements during orthogonal cutting conditions. It is found that a change in the positive direction of α_r gives a reduction of the cutting forces. This was also shown by experimental measurements in [11]. Both results from finite elements and experiments show that the analytical expressions derived from mechanistic models [12, 13, 14] are valid for orthogonal cutting conditions. There-

2212-8271 © 2018 The Authors. Published by Elsevier B.V.
Peer-review under responsibility of the Scientific Committee of the 15th CIRP Conference on Computer Aided Tolerancing - CIRP CAT 2018.
10.1016/j.procir.2018.04.029

fore it is crucial to control any geometric variation in the interface between the tool body and carbide insert, that can affect key characteristics of the cutting tool such as cutting point, rake angle and tool life.

An approach is needed to identify sensitive contact areas on a surface between two or more contacting bodies with respect to any systems key characteristics. In this paper a methodology will be presented on a industrial application using a parting tool in orthogonal cutting conditions, Corocut QD tool and QD-NE-0200-0502-CM carbide insert. The proposed method is divided in two separate parts, FEA and variational simulation. In the FEA part a test space is created using design of experiments, where the independent variables are geometric variations of the contact surface and the response is the stress magnitude in each individual node in the contact surface. Each observation is simulated and the results from the contact surfaces are extracted. In order to perform the variational simulation a meta-model is created for each individual node of the contact surface. This allows for a larger data set to be simulated within the boundaries of the test space also the independent variables are not bound to a specific distribution.

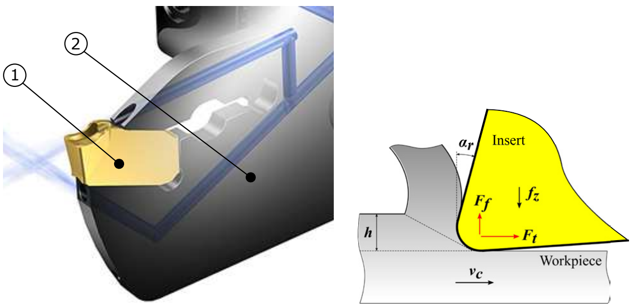

(a) Cutting tool assembly [15], **1** - carbide insert, **2**-tool body

(b) Illustration of the cutting process

Fig. 1: Corocut QD cutting tool

1.1. Scope of Paper

The aim of this paper is to present an approach that can handle contact variation in surface-to-surface contacts with external loads. The methodology will be presented using an industrial case from the machining industry where these conditions are common. The relationship between contact variation and the rake angle of the cutting tool is investigated and the goal is to minimize its impact on the rake angle. The main approach of the methodology is to create a sample space of geometric variations on the tool body in the interface to the carbide insert. Output from this paper will be the effect from geometric variations in the contact surface on cutting forces. One may decide tolerances based on minimizing the variation of the cutting forces due to geometric variations in the interface during a metal removal process or similar problem definitions. Results based upon the presented methodology are valuable input for tolerance allocation of both the surface geometry and functional requirements such as rake angle.

In Section 2.1 the industrial case is presented and the input parameters for the meta-model that are described in Section 2.4. The FE model is presented in Section 2.3 and the analysed rake angle variation and how it effects the cutting forces are modelled in Section 2.2. The results of the methodology are presented in Section 3 and conclusions are drawn in Section 4.

2. Methodology

The aim of the methodology is to create a set of tools in order to set suitable functional tolerance requirements for surface-to-surface contacts under external loads. The main activities are presented in a flowchart, see Fig. 6.

The first step is to create a test space to cover all possible combinations of the input variables. Afterwards FEA is used to simulate the cutting process during steady state conditions, meaning, the entry and exit from the workpiece are neglected and the cutting forces are stable. The variational simulations are performed by building meta-models of the stress distributions in the contacting surfaces. This allows for faster simulations outside the FE environment.

2.1. Generation of the Test Space

To create the test space Latin Hypercube Sampling (LHS) [16, 17] with a uniform distribution is used. A uniform LHS partitions the parameters evenly into Latin squares, where the parameter can only take a value once within a Latin square. One draw back of using LHS is that extreme values, on parameter limits, will most likely not be captured. To resolve this issue the LHS is combined with a 2-level full factorial sampling. In [18] the author suggests that $15 - 25$ observations per variable are needed for a linear regression model. For this paper, 30 observations per variable are used. This is done because some design points may not converge due to the complex contact formulation and to pick up any non-linear behaviours.

The interface between the tool body and insert contains eight surfaces that are in contact, each surface has six degrees of freedom, see Fig. 2a - 2e. This means that the assembly has 48 degrees of freedom (24 for the insert, 24 for the tool). In order to get a reliable meta-model, according to [18], a total of 1440 design points need to be simulated. This requires an excessive amount of computer resources, therefore the model needs to be reduced without loosing valuable information.

The tool body has three separate contact surfaces, $s = 1, 2, 3$, and each surface has its own local coordinate system ($LCS^{(s)}$), see Fig. 2a. The insert is assumed to be nominal and rigid since not enough information exists on how the surfaces vary in the insert. It is also assumed that the tool is symmetric in the YZ-plane and that the back support, in the local coordinate system $LCS^{(1)}$, only translates along its y-axis.

With these simplifications, the model now has 10 input parameters, which will give 300 design points to simulate. In Fig. 2 each contacting surface and its degrees of freedom are visualised. The parameters are also presented in Table 1 together with their lower and upper tolerance limits. The superscript of the parameters in the first column of Table 1 denotes which surface it belongs to ($s = 1, 2, 3$), see Fig. 2a. The first value of the subscript denotes if it is a translational (T) degree of freedom or rotational (R) degree of freedom. The second value of the subscript denotes around or along which local coordinate axis it is bound to, see Fig. 2b. - 2e. It should be noted that due to confidentiality the used tolerances are arbitrary and are not representing the real variation.

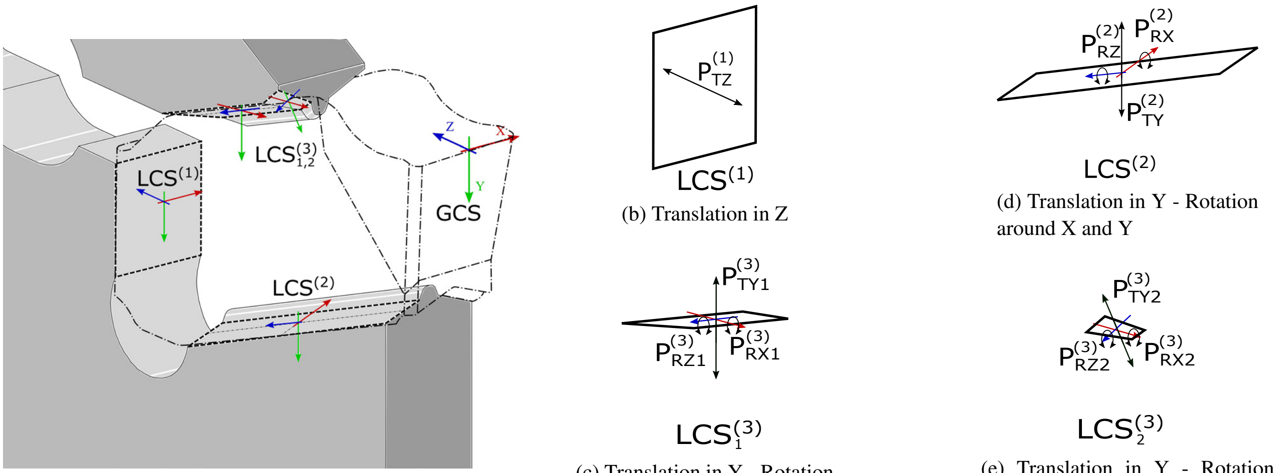

(a) Contact surfaces of the tool body

(b) Translation in Z

(c) Translation in Y - Rotation around X and Y

(d) Translation in Y - Rotation around X and Y

(e) Translation in Y - Rotation around X and Y

Fig. 2: Contact surface degree of freedom

Table 1: Parameters with nominal value and variation

Parameter	**Lower boundary**	**Nominal**	**Upper Boundary**	**Unit**	**DOF**	
$P_{TZ}^{(1)}$	−0.01	0	0.01	mm	Translation	$Z^{(1)}$-axis
$P_{RX}^{(2)}$	−1	0	1	deg	Rotation	$X^{(2)}$-axis
$P_{RZ}^{(2)}$	−1	0	1	deg	Rotation	$Z^{(2)}$-axis
$P_{TY}^{(2)}$	−0.01	0	0.01	mm	Translation	$Y^{(2)}$-axis
$P_{RX1}^{(3)}$	−1	0	1	deg	Rotation	$X^{(3)}$-axis
$P_{RZ1}^{(3)}$	−1	0	1	deg	Rotation	$Z^{(3)}$-axis
$P_{TY1}^{(3)}$	−0.01	0	0.01	mm	Translation	$Y^{(3)}$-axis
$P_{RX2}^{(3)}$	−1	0	1	deg	Rotation	$X^{(3)}$-axis
$P_{RZ2}^{(3)}$	−1	0	1	deg	Rotation	$Z^{(3)}$-axis
$P_{TY2}^{(3)}$	−0.01	0	0.01	mm	Translation	$Y^{(3)}$-axis

2.2. *Cutting Force Model*

The empirical model derived by Kienzle [19] is chosen to model the tangential force, F_t, and the axial feed force, F_f, since it gives a good prediction for large variation in chip thickness, see Fig 1b. The model takes the effects from strain hardening of the workpiece material, induced in the previous revolution, into consideration. It is also the most commonly used model to predict cutting forces and cutting energy. Kienzle introduced the specific cutting coefficients (m_c, K_{c1}, m_f and K_f) which describes the amount of force required to remove material from the workpiece with a specific insert geometry. The forces are given by:

$$F_t = K_{c1} a_p h^{1-m_c} \tag{1}$$

$$F_f = K_f a_p h^{1-m_f} \tag{2}$$

where K_{c1} is the specific cutting force in tangential direction. The tool-workpiece dependent exponent of the tangential force, m_c, describes the behaviour of the cutting force in different materials. K_f is the specific feed force and m_f is the tool-workpiece dependent exponent of the feed force. The cutting forces are measured empirically at different feed rates, f_z. The cutting depth h is in the same direction as the feed and therefore it is directly connected to the feed and can be formulated as $h = f_z$, where f_z is the feed in axial direction. For an arbitrary parting operation the feed f_z is chosen as 0.2 mm/rev. The cutting width a_p is determined by the width of the insert and for the chosen tool the cutting width is 3 mm. The numerical values for the modelled cutting coefficients for the combination of $SS\,2541$ workpiece material and Corocut $QD - NE - 0200 - 0502 - CM$ insert are $m_c = 0.22$, $K_{c1} = 1745\text{N/mm}^2$, $m_f = 0.47$ and $K_f = 605\text{N/mm}^2$. From empirical studies done by AB Sandvik Coromant it is found that 1° change in the rake angle give 1% change in the tangential force F_t and a 4% change in the feed force F_f. Assuming that this relationship is reasonable a linear variation term $\{1 - p_{t,f}\delta_{\alpha_r}\}$ is added to the Kienzle's force model Eqn.(1)-(2). Where p_t and p_f are amplification constants ($p_t = 0.01$ and $p_f = 0.04$) for the rake angle variation δ_{α_r}:

$$F_t = K_{c1} a_p f_z^{1-m_c} \{1 - p_t \delta_{\alpha_r}\} \tag{3}$$

$$F_f = K_f a_p f_z^{1-m_f} \{1 - p_f \delta_{\alpha_r}\} \tag{4}$$

Sign convention of δ_{α_r} gives that a $\delta_{\alpha_r} < 0$ results in a more negative rake angle which increases cutting forces, while $\delta_{\alpha_r} > 0$ gives an increased positive rake angle and reduced cutting forces [10, 11].

2.3. Finite Element Model

The finite element analysis is done with the commercial software Ansys®. The entire tool model consists of linear solid elements (*SOLID185*), with contact elements (*CONTA174*) on the contact surfaces (tool body) where the insert has *TARGE170* target elements, meaning that the contact methodology is surface-to-surface which is solved with an unsymmetric Newton-Raphson method. The insert is assumed to be rigid in relation to the tool body, since Corocut QD – NE – 0200 – 0502 – CM has a grade 1125 and is PVD-coated (Physical Vapor Deposition) with a $(Ti, Al)N$ composition. This gives a compressive yield strength significantly higher than the tool material ($SS2541$). A friction coefficient for contact between carbide and steel is chosen according to [20] as $\mu = 0.5$ in order to give a more realistic movement of the insert in the tip seat. The used material model for the tool body is a linear in-built steel model with Young's modulus given as $E = 200$ GPa and Poisson's ratio as $\nu = 0.3$.

For each observation and simulation a CAD (Computer Aided Design) model is generated where the geometry of the interface deviate from its nominal values. This will cause the contacting surfaces $LCS^{(3)}_{1,2}$, Fig. 2c - 2e, to penetrate the insert surface. The contact search algorithm adds a displacement in the normal direction of the contact elements, allowing the tool to open. Only the self clamping finger ($LCS^{(3)}_{1,2}$) is allowed to move in order to avoid any unrealistic deformations due to the contact search algorithm. Once all contacts are found with no penetration, the rigidity in the finger pushes the carbide insert down, locking it in place.

In the simulations the adaptor connecting the tool to machine is neglected. The interface between the adaptor and tool body is seen as rigid with no flexibility thus locking all degrees of freedom with an overhang of 50 mm. The cutting force is applied on the tip of the insert at $(0, 0, 0) \in GCS$, see Fig. 2a, in over the whole width with a depth of 0.2 mm corresponding to a feed of 0.2 mm/rev. The magnitude of the cutting forces are found to be $F_y = 1493$ N, $F_z = 773$ N and are experimentally retrieved by Sandvik Coromant. The carbide insert is prohibited to translate in the X-direction and rotate around Y and Z axes , meaning it can only translate in the YZ-plane of the global coordinate system GCS, see Fig. 2a.

2.4. Meta-Model

To analyse variation a meta-model relating tolerances to stress concentrations is designed with a second-order function with interaction terms.

$$\ln(\mathbf{Y}^{(s)}_i) = \boldsymbol{\beta}^{(s)}_0 + \sum_{j=1}^{r} \boldsymbol{\beta}^{(s)}_j \mathbf{X}^{(s)}_{i,j} + \epsilon^{(s)}_i, \quad \text{for } i \leq r \tag{5}$$

The function is built in such that each node on the contact surface has its own meta-model. Due to the over-constrained assembly, some design points may have one node with equivalent stresses around 1 GPa and in the next design point it is 0. The variation in the stress magnitudes can cause a poor fit between the simulated data and the meta-model. Therefore the nodal response, $\mathbf{Y}^{(s)} \in \mathbb{R}^{r \times n^{(s)}}$, is logarithmic, where r is the number of design points or observations and $n^{(s)}$ is the number of nodes for the surface s. The matrix $\mathbf{X} \in \mathbb{R}^{r \times (1+m)}$ is a matrix containing all terms of the 2^{nd}-order polynomial where m is the number of independent variables, and a column of ones to give the β_0 terms for each observation. The matrix $\boldsymbol{\beta}^{(s)} \in \mathbb{R}^{(1+m) \times n^{(s)}}$ is a matrix of the coefficients in the regression model and $\epsilon^{(s)} \in \mathbb{R}^{r \times n^{(s)}}$, defined by $\epsilon^{(s)} = \mathbf{Y}^{(s)} - \hat{\mathbf{Y}}^{(s)}$, is the matrix of residuals between the true response and the predicted response [21]. The model is then fitted by using least squares and finding the minimum vertical distance between the data points and polynomial line.

2.5. Variation Simulation Using a Meta-Model

The variation simulations are conducted using Direct Monte Carlo (DMC) simulations with the nodal meta-model, Eqn. 5. The input variables, Table 1, are randomly generated for each monte carlo simulations. In order to achieve a contact the magnitude of the stress in a node needs to be equal or exceed the compressive yield stress, $\sigma_c = 250$ [MPa], so called full contact. This gives the expression of the probability of full contact for a node i on the contacting surfaces of the tool body.

$$p_{fc}{}^{(s)}_i = \sum_{k}^{N} \frac{(\phi_i)^{(s)}_k}{N} \tag{6}$$

$$\phi^{(s)}_i = \begin{cases} 1 & \text{if } \hat{Y}^{(s)}_i \geq 250\text{MPa} \\ 0 & \text{else} \end{cases} \tag{7}$$

The number of DMC simulations is $N = 1000$ and the number of nodes on a contacting surface. $s = 1, 2, 3$, is given by $n^{(s)}$.

3. Results

To illustrate the application of the methodology a parting tool from the machining industry is used thus it fulfils the sought requirements of surface-to-surface contacts and an external load. In order to define a contact, the concept of full contact has been used. In order to minimize the computer resources used, the number of independent variables was reduced as described in Section 2.1. This resulted in four surfaces moving independent of each other thus giving an indirect effect on the rake angle dependent on the contact variation. The geometric variations are controlled through the CAD software where each surface is seen as a plane with at maximum six degrees of freedom.

3.1. Comparison Between Variation in the Fitted Model and the FE-model

The variation simulation is done by DMC with a randomly distributed sample space within the specified boundaries given in Table 1 for the fitted model. The surface plots in Fig. 3 show the probability of a full contact in a particular region for the

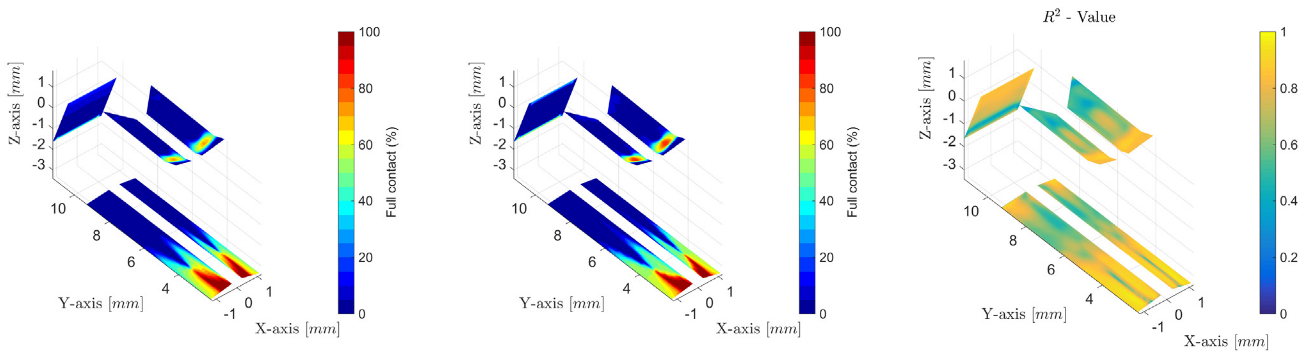

(a) Variational model for 1000 DMC iterations using the meta-model

(b) FE-model with r observations

(c) R^2-value plotted over the surfaces of the tip seat

Fig. 3: Probability of full contact on the tip seat

Table 2: Maximum and minimum values of the variation due to the rake angle variation, δ_{α_r}

Parameter			**Unit**
δ_{α_r}	−0.55	1.32	deg
$F_f(\delta_{\alpha_r})$	791	732	N
$F_t(\delta_{\alpha_r})$	1500	1472	N

meta-model and for the FEA. Here, full contact is equivalent to stresses equal to, or exceeding the compressive yield strength. This means that for the bottom surface, roughly 40% of the production outcomes will have contact close to the YZ-plane or close to the sides of the parting tool. Where the contact is located will have an effect on the deformation of the surface which in turn will affect the rake angle of the insert under operation.

3.2. Correlation Between Tolerances and Responses

In Fig. 4 a correlation between the input tolerances and the response, the effective stress, is shown over the surfaces of the tip seat. It can be seen that parameter $P^{(2)}_{RZ}$ has the most influence on the stress in the bottom surface (s = 2). On the back surface (s = 1) there is a field where the most significant parameter is $P^{(3)}_{TY1}$, which is unlikely. By observing the R^2-value in Fig. 3c the same field has a R^2-value of approximately 0.3 which shows a poor correlation with the FE-data. Therefore $P^{(3)}_{TY1}$ is not taken in to consideration for the adjustment of tolerances. It should be noted that there can exist cases where one parameter can have a 51% influence while another parameter have 49% and these are not taken into consideration. .

3.3. Variation Simulation with Adjusted Tolerances

It was found that $P^{(2)}_{RX}$ and $P^{(2)}_{RZ}$ and $P^{(3)}_{RZ1}$ had the most influence on the stress location and magnitude. By looking at their definition in the CAD-model, one can see that by changing the parameters from symmetric to positive asymmetric tolerances, contact variation is localized as seen in Fig. 3. The parameters are presented in Table 3 and the remaining parameters are kept the same. The probability for full contact can be seen in Fig. 5 for the tolerances defined in Table 3. In Table 4 the rake angle

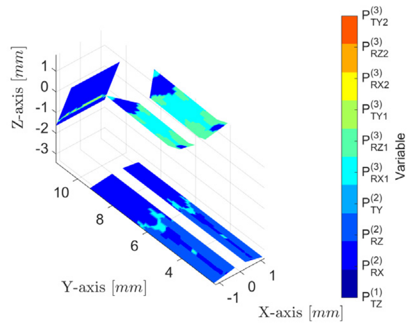

Fig. 4: Parameters with most correlation to the surface stresses

variation and force variation are presented with the new set of tolerances.

Table 3: Parameters with nominal value and upper/lower limits

Parameter	**Lower boundary**	**Nominal**	**Upper Boundary**	**Unit**
$P^{(2)}_{RX}$	0	0.5	1	deg
$P^{(2)}_{RZ}$	−0.8	−0.65	−0.5	deg
$P^{(3)}_{RZ1}$	0	0.5	1	deg

Table 4: Maximum and minimum values of the variation due to the rake angle variation, δ_{α_r}, with adjusted tolerances

Parameter			**Unit**
δ_{α_r}	−0.42	−0.08	deg
$F_f(\delta_{\alpha_r})$	787	776	N
$F_t(\delta_{\alpha_r})$	1498	1493	N

4. Conclusion

The proposed methodology was proven to be very successful in redefining the tolerances within the test space and finding the most influential parameters. Due to the fact that the method is based on FEA it can be applied on any situation where a finite element model can be provided and operational conditions are known, though further case studies needs to be done to confirm this. The methodology can be divided into four major steps (1) create a sample space using design of experiments, (2) simulate the test space using FEA, (3) build the meta-model for each node on the contacting surfaces and (4) optimize the contact variation.

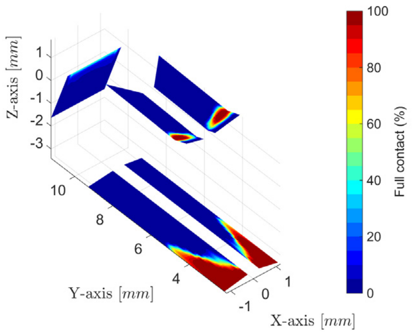

Fig. 5: Probability of full contact on the tip seat

A more detailed work process can be seen in Fig. 6 in the form of a flow chart. By following the developed methodology it was found that (1) three parameters had significant effects on the contact variations, see in Table 3 and (2) the rake angle was only dependent on $P^{(2)}_{RZ}$, the rotation of the bottom surface around its z-axis.

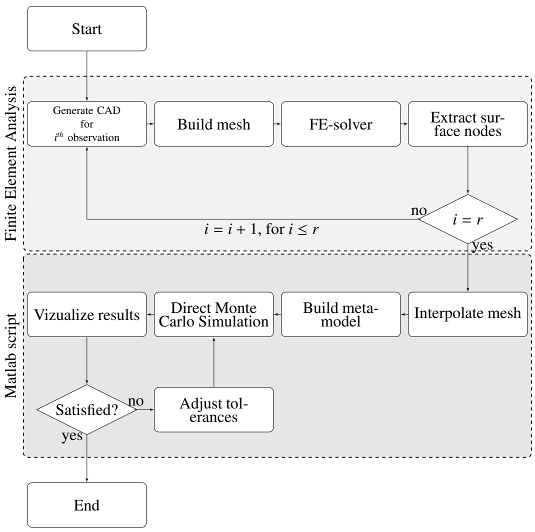

Fig. 6: Flow chart for the presented methodology to determine tolerances in early product development

The obtained results imply that variation simulations can be conducted for complex geometries where contact points are not known for systems under external forces, for example metal cutting operations. The finite element model and its surfaces variations have not been validated against physical experiments with respect to geometric variations, however for this paper the presented finite element model should be seen as a proof of concept. It is shown in Fig. 3c, that the meta-model was able to pick up and replicate the significant areas. This is assumed to be where the majority of the contact is located. The downside of using meta-models fitted with least squares is that it does not take outliers into consideration which can be of importance for over-constrained assemblies.

For future work it might be interesting to consider (1) validation of the finite element model, (2) how to optimize contact location with respect to robustness and key characteristics and (3) how to incorporate time variant deviations in the cutting process.

5. Acknowledgement

This work was carried out at the Wingquist Laboratory within the Area of Advance Production at Chalmers, supported by the Swedish Governmental Agency for Innovation Systems (VINNOVA). The support is gratefully acknowledged. A deep gratitude goes towards the department of Metal Cutting Modelling at AB Sandvik Coromant for the help and support.

References

[1] Wang, H., Rong, Y.K., Li, H., Shaun, P.. Computer aided fixture design: Recent research and trends. Computer-Aided Design 2010;42(12):1085–1094.
[2] Söderberg, R., Lindkvist, L.. Computer Aided Assembly Robustness Evaluation. Journal of Engineering Design 1999;10(2):165–181.
[3] Cai, W., Hu, S.J., Yuan, J.X.. Deformable Sheet Metal Fixturing: Principles, Algorithms, and Simulations. Journal of Manufacturing Science and Engineering 1996;118(3):318.
[4] Söderberg, R., Lindkvist, L., Dahlström, S.. Computer-aided robustness analysis for compliant assemblies. Journal of Engineering Design 2006;17(5):411–428.
[5] Schleich, B., Wartzack, S.. A discrete geometry approach for tolerance analysis of mechanism. MAMT 2014;77:148–163.
[6] Liu, S.C., Hu, S.J.. Variation Simulation for Deformable Sheet Metal Assemblies Using Finite Element Methods. Journal of Manufacturing Science and Engineering 1997;119(3):368.
[7] Lorin, S., Söderberg, R., Carlson, J., Edelvik, F.. Simulating Geometrical Variation in Injection Molding. In: International Conference on Methods and Tools for Product and Production Development; vol. Aug. 25-27. Göteborg; 2010,.
[8] Lorin, S., Lindkvist, L., Söderberg, R.. Simulating Part and Assembly Variation for Injection Molded Parts. In: International Design Engineering Technical Conferences & Computers and Information in Engineering Conference. Chicago; 2012,.
[9] Jayaprakash, G., Sivakumar, K., Thilak, M.. Parametric Tolerance Analysis of Mechanical Assembly Using FEA and Cost Competent Tolerance Synthesis Using Neural Network. J Software Engineering & Applications 2010;3:1148–1154.
[10] Shih, A.J.. Finite element analysis of the rake angle effects in orthogonal metal cutting. International Journal of Mechanical Sciences 1995;38(1):1–17.
[11] Günay, M., Korkut, I., Aslan, E., Seker, U.. Experimental investigation of the effect of cutting tool rake angle on main cutting force. Journal of Materials Processing Technology 2005;166(1):44–49.
[12] Altintas, Y.. Manufacturing Automation: Metal cutting mechanics, machine tool vibrations, and CNC design. 2nd ed.; New York: Cambridge University Press; 2012.
[13] Shaw, M.C.. Metal Cutting Principles. Oxford: Claredon Press; 1989.
[14] Stephenson, D.A., Agapiou, J.S.. Metal Cutting Theory and Practice. New York: Marcel Dekker; 1997.
[15] CorocutQD, . AB Sandvik Coromant. 20180306. URL: `https://www.sandvik.coromant.com/en-us/products/corocut-qd`.
[16] Stein, M.. Large Sample Properties of Simulations Using Latin Hypercube Sampling. Techometrics 1987;29(2).
[17] Mckay, M.D., Beckman, R.J., Conover, W.J.. A Comparison of Three Methods for Selecting Values of Input Variables in the Analysis of Output from a Computer Code. Techometrics 1979;21(2):239–245.
[18] Green, S.. How Many Subjects Does It Take to Do a Regression Analysis? MULTIVARIATE BEHAVIORAL RESEARCH 1991;26(3).
[19] Kienzle, O., Victor, H.. Spezifische Schnittkrafte bei der Metallbearbeitung. Werkstofftechnik und Machinenbau 1957;45(7):224–225.
[20] Holmberg, K., Matthews, A.. Coatings Tribology: Properties, Mechanisms, Techniques and Applications in Surface Engineering. Elsevier; 2009.
[21] Draper, N.R., Smith, H.. Applied Regression Analysis. 3rd ed. ed.; New York: John Wiley & Sons, INC; 1998.